Journal of Marine Science and Technology
https://doi.org/10.1007/s00773-024-01018-y

ORIGINAL ARTICLE

Automatic docking with extended dynamic positioning

Stefan Larsen[1,2] · Håkon Hagen Helgesen[1,2] · Jens Emil Walmsness[1,2] · Giorgio Kwame Minde Kufoalor[2] · Tor Arne Johansen[1]

Received: 16 May 2023 / Accepted: 25 July 2024

Abstract
This article presents an automatic docking method suitable for fully actuated surface vessels for the purposes of assisting operators of maritime vessels when docking in time-varying environmental conditions. Docking of ships is a particularly stressful task for human operators, with high demands for both speed and precision, especially under influence from environmental disturbances such as wind, waves and ocean currents. The need for automatic docking systems is increasing as unmanned maritime vessels become more advanced and integrated into global maritime transportation. To address this task, a comprehensive automatic docking algorithm was developed, with path following and velocity control using a modified dynamic positioning control system, which makes the method applicable in existing industrial control systems. In addition, the method includes capability analysis of the docking procedure and evaluates strategies for counteracting disturbances. Specifically, this method utilizes a modified dynamic positioning control system using position sensor data only, to control position, heading and velocity in different stages when docking automatically. The methods are proven in simulations and field experiments.

Keywords Unmanned surface vehicle · Docking · Dynamic positioning · Dynamic positioning capability

1 Introduction

Docking is a critical part of ship operations, and many accidents occur during docking and harbor maneuvering [1–3]. The reduced maneuverability at low speed together with increased influence from environmental forces and hydrodynamic effects near the dock are significant challenges that human operators must overcome [4]. Moreover, the environment might include geometric constraints and several static and dynamic obstacles that must be avoided while planning the docking maneuver [5, 6]. These factors make a docking maneuver a particularly stressful task for human operators, and it is not uncommon that an operator needs several attempts to dock a ship in challenging conditions. Developing automatic systems for docking is, therefore, an interesting research topic that fits well into the current state of maritime research where safer and greener operations are important goals for the future fleet of unmanned and manned ships [7, 8].

This article addresses automatic docking control for surface vessels, which requires solutions to several topics within the general structure of guidance, navigation and control [9]. It is assumed that the vessel has an accurate navigation system that provides state estimates to the control system [9, Chapter 13–14]. Control allocation is outside the scope of this article, and it is assumed that the desired control forces are mapped appropriately to the actuators.

Control systems for automatic docking are often based on two different mindsets even though the low-level controller structure might be similar. The first approach is based on conventional linear or nonlinear PID controllers that are used to track specific reference signals determined by a reference filter or a human operator. This is often inspired by dynamic positioning (DP) approaches where the low-speed assumptions in DP are utilized to conduct docking maneuvers at low speed while maintaining position and heading control [5, 10]. These methods require a guidance system that is tailored to provide reasonable references when used

✉ Stefan Larsen
stefan.larsen@inria.fr

[1] Department of Engineering Cybernetics, Norwegian University of Science and Technology, O. S. Bragstads plass 2D, 7491 Trondheim, Norway

[2] Maritime Robotics AS, Brattørkaia 11, 7010 Trondheim, Norway

Published online: 24 August 2024

in docking. The method presented in this article falls into this category.

The second category is based on optimization and contains several different methodologies. A common denominator is a higher-level path-planning system that calculates an optimal docking path with respect to some criterion, for example, energy consumption, time or distance. Docking systems in this category are typically based on reinforcement learning [11–13], artificial neural network [14–17] or model-predictive control (MPC) [18].

Docking of surface ships has been studied recently as exemplified in the previous paragraph. However, there are shortcomings in the literature and one could argue that there exist more literature on docking for underwater vehicles [19–22]. Few works present computational effective and flexible optimization-free methods that have been validated experimentally for surface vessels. It is desirable to develop docking control systems that do not require real-time solutions to computationally demanding optimization problems. The main reason is that these systems are more prone to failures due to unknown disturbances or computational issues. Moreover, using an optimization-free strategy requires less added complexity on existing vessels and enables a simple adaptable docking method for vessels with already implemented DP control systems. How conventional DP systems can be modified and used in docking is not addressed thoroughly in existing literature. This work seeks to address some of these shortcomings by developing a simple but effective docking control system that is flexible and generalizable to multiple vessels and locations.

Counteracting and mitigating the local environmental effects from wind, waves and ocean currents are important for the docking performance. Wind forces can, for example, push the vessel sideways and the control system must compensate for these forces to dock at the correct location. Consequently, the controller reference signals should ideally be adapted to the local environmental effects to improve the robustness. It is possible to measure the environmental forces from wind and ocean current directly but it requires additional equipment on the quay or the vessel. An alternative is to estimate the environmental forces to identify external forces that do not fit into a traditional low-speed maneuvering model, but this requires a vessel model. Nevertheless, measurements or estimates of the speed and direction of external forces can be used in the control design to plan the docking path on the fly, as discussed in the results of this docking procedure.

The effects of environmental forces can also determine the capabilities of the automatic docking method. The docking capability is defined as the ability to have a position and heading within a specific region during docking, when exposed to environmental forces from any angle. Such a capability analysis is inspired by dynamic positioning capability analysis for station-keeping [23], and will be extended and simplified for the case of docking in this work. If the environmental forces are observed to be greater than the basic capabilities of the docking control system, alternative strategies can be activated to avoid critical situations.

The work with most resemblance to this article presented a path-following system for surface vessels based on speed and heading control using a propeller and rudder [24]. However, how DP can be used in docking and the capability of their method are not described in detail. Moreover, direct sway control is not possible with their chosen actuator setup. Consequently, this article provides additional insight into how automatic docking can be conducted using optimization-free control methods for a fully actuated vessel.

Standard DP control systems could be used for the entire docking procedure, however this is undesirable with respect to speed and precision. As standard DP systems only use a position reference, they only have indirect control of speed and acceleration. This might cause unwanted maneuvers and less control when making contact with the quay. These are particularly critical aspects in narrow ports to avoid collisions and to not block the path of other vessels, while streamlining the ship operation. This motivates the need for direct control of speed and thrust when using DP to perform safe and time-efficient docking.

The main contribution of this article is a flexible and modular docking control system with experimental verification, that can steer the vessel to the dock automatically while compensating for the local environmental effects and assessing the capability of the vessel. It is designed as a general motion planning concept, and assumes that the vessel is fully actuated in the plane. The proposed control system is inspired by a traditional DP system and how human operators control the vessel during docking. The minor modifications introduced to traditional DP, for direct control of speed and thrust in the final phases, make this proposed docking method easily adaptable to existing industrial DP systems.

The remainder of this article is divided into six sections. Section 2 describes mathematical models for vessel motion and control that are used in this work. Section 3 describes the proposed docking method and the transitions between the different phases. Section 4 describes the capability analysis and a possible strategy when the capability is challenged by environmental forces. The experimental design is presented in Sect. 5, while the results and discussions are presented in Sect. 6. The article is concluded in Sect. 7.

2 Background

This section presents mathematical models used for simulation and design of the different modules. This includes coordinate frames, kinematics, the dynamic model used to represent the

surface ship, and models for the environmental forces. The latter part looks into DP and guidance.

2.1 3 DOF maneuvering model for ship

The motion of surface ships is typically modeled in three degrees of freedom (DOF) where roll, pitch and heave are neglected. This is a fair simplification for vessels that are metacentrically stable with sufficient damping in roll, and when disregarding extreme weather conditions.

A local tangent plane is used for local positioning, the North-East-Down (NED) frame, denoted $\{n\} = (x_n, y_n, z_n)$. It is normally assumed that $\{n\}$ is inertial, neglecting the rotation and curvature of the Earth. Fixed to the maritime craft is the BODY frame denoted $\{b\} = (x_b, y_b, z_b)$, where the x_b axis goes from aft to fore, y_b goes from port to starboard and z_b goes from deck to keel [25].

The coordinate frames in the horizontal plane are illustrated in Fig. 1 inspired by [9, Chapter 2].

The generalized position (pose) vector is defined as

$$\boldsymbol{\eta} = \begin{bmatrix} x^n & y^n & \psi \end{bmatrix}^\top \in \mathbb{R}^3, \tag{1}$$

where x^n is the north position, y^n is the east position, and ψ is the heading angle. The heading ψ equals the course angle χ minus the crab angle β_c. Given ocean current encounter angle γ_c, the velocity, relative velocity and ocean current velocity are $\boldsymbol{\nu}$, $\boldsymbol{\nu}_r$ and $\boldsymbol{\nu}_c$, respectively, and they are defined in the body frame as

$$\boldsymbol{\nu}^b = [u \quad v \quad r]^\top \in \mathbb{R}^3, \tag{2a}$$

$$\boldsymbol{\nu}_c^b = \begin{bmatrix} u_c & v_c & 0 \end{bmatrix}^\top \in \mathbb{R}^3, \tag{2b}$$

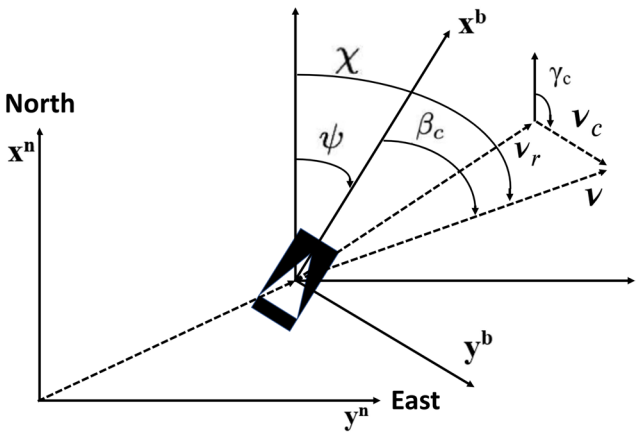

Fig. 1 Horizontal plane of NED and BODY coordinate frames, and the ocean current triangle

$$\boldsymbol{\nu}_r^b = \boldsymbol{\nu}^b - \boldsymbol{\nu}_c^b = \begin{bmatrix} u_r & v_r & r_r \end{bmatrix}^\top \in \mathbb{R}^3. \tag{2c}$$

Since the ocean current is considered irrotational and constant in $\{n\}$, r_c is zero as specified in (2b).

A common 3 DOF nonlinear maneuvering model for simulation of surface vessels, influenced by environmental forces from wind, waves and ocean current, is given by [9, Chapter 6]

$$\dot{\boldsymbol{\eta}} = \boldsymbol{R}_b^n(\psi)\boldsymbol{\nu}, \tag{3a}$$

$$\boldsymbol{M}\dot{\boldsymbol{\nu}}_r + \boldsymbol{N}(\boldsymbol{\nu}_r)\boldsymbol{\nu}_r = \boldsymbol{\tau} + \boldsymbol{\tau}_{\text{wind}} + \boldsymbol{\tau}_{\text{wave}}. \tag{3b}$$

See Appendix A for numerical values used in this article.

The rotation matrix $\boldsymbol{R}_b^n(\psi)$ defines the principal rotation between $\{n\}$ and $\{b\}$, and is expressed in 3 DOF as

$$\boldsymbol{R}_b^n(\psi) = \begin{bmatrix} \cos(\psi) & -\sin(\psi) & 0 \\ \sin(\psi) & \cos(\psi) & 0 \\ 0 & 0 & 1 \end{bmatrix}. \tag{4}$$

The mass matrix in (3b) is defined as $\boldsymbol{M} = \boldsymbol{M}_{RB} + \boldsymbol{M}_A$, where $\boldsymbol{M}_{RB}$ is the rigid-body mass matrix, and $\boldsymbol{M}_A$ is the added mass matrix. The nonlinear damping matrix $\boldsymbol{N}(\boldsymbol{\nu}_r)$ is defined as

$$\boldsymbol{N}(\boldsymbol{\nu}_r) = \boldsymbol{C}_{RB}(\boldsymbol{\nu}_r) + \boldsymbol{C}_A(\boldsymbol{\nu}_r) + \boldsymbol{D}(\boldsymbol{\nu}_r), \tag{5}$$

where $\boldsymbol{C}_{\text{RB}}(\boldsymbol{\nu}_r)$ is the rigid-body Coriolis and centripetal matrix, $\boldsymbol{C}_A(\boldsymbol{\nu}_r)$ is the added mass Coriolis and centripetal matrix, and $\boldsymbol{D}(\boldsymbol{\nu}_r)$ is the hydrodynamic damping matrix. However, for low-speed maneuvering that is encountered in docking, the Coriolis matrices are close to zero, and the damping matrix becomes constant, so the simplified maneuvering model has $\boldsymbol{N}(\boldsymbol{\nu}_r) = \boldsymbol{D}$ and only consists of linear damping. Finally, the remaining forces and moments for control, wind and waves are denoted by $\boldsymbol{\tau} \in \mathbb{R}^3$, $\boldsymbol{\tau}_{\text{wind}} \in \mathbb{R}^3$, and $\boldsymbol{\tau}_{\text{wave}} \in \mathbb{R}^3$, respectively. The ocean current is included through the relative velocity $\boldsymbol{\nu}_r$.

2.2 Environmental forces and moments

Given wind speed V_w and wind encounter angle γ_w, like the ocean current angle γ_c illustrated in Fig. 1, the generalized wind forces in 3 DOF acting on a surface vessel moving at relative speed V_{rw} are defined as [9, Chapter 10]

$$\boldsymbol{\tau}_{wind} = \frac{1}{2}\rho_a V_{rw}^2 \begin{bmatrix} C_X(\gamma_w)A_{F_w} \\ C_Y(\gamma_w)A_{L_w} \\ C_N(\gamma_w)A_{L_w}L_{oa} \end{bmatrix}. \tag{6}$$

The wind model is given by the wind coefficients $\boldsymbol{C} = [C_X, C_Y, C_N]$ with mass density of air ρ_a, centroids above the water line of the projected areas $\boldsymbol{A} = [A_{F_w}, A_{L_w}]$, and the overall length L_{oa} of the vessel. The wind coefficients

$\boldsymbol{C}$ can be computed from a simple load concept based on Helmholtz–Kirchhoff plate theory [9, Chapter 10].

The total wave force is defined as $\boldsymbol{\tau}_{\text{wave}} = \boldsymbol{\tau}_{\text{wave1}} + \boldsymbol{\tau}_{\text{wave2}}$. The first-order wave-induced forces $\boldsymbol{\tau}_{\text{wave1}}$ consist of the zero-mean oscillatory motions while the second-order wave-induced forces $\boldsymbol{\tau}_{\text{wave2}}$ are the slowly-varying nonzero drift components. Given the encounter angle β_w, like the ocean current crab angle β_c illustrated in Fig. 1, the first-order wave-induced forces that may appear in confined waters and ports, known as wake forces, are described as [9]

$$\boldsymbol{\tau}_{\text{wave1}} = \boldsymbol{R}_n^b(\psi) \begin{bmatrix} W_x^n(t) \\ W_y^n(t) \\ W_\psi(t) \end{bmatrix} = \begin{bmatrix} W^n(t)\cos\beta_w \\ W^n(t)\sin\beta_w \\ W_\psi(t) \end{bmatrix}. \tag{7}$$

To simulate the practical effects of the oscillations from wake waves, a simplification of the form and magnitude of the forces $W^n(t)$ and $W_\psi(t)$ is modeled as a sine wave function, on the form

$$W(t) = Ae^{-at}\cos(ft + \phi) + Be^{-bt}. \tag{8}$$

The second-order wave-induced forces $\boldsymbol{\tau}_{\text{wave2}}$ are modeled as three slowly-moving random walk processes with a zero-mean Gaussian white noise process as input w_{d_i}, with standard deviation $\boldsymbol{\sigma}_{\text{wave}}$ [9]

$$\begin{aligned} &\dot{d}_i = w_{d_i}, \quad i \in \{1, 2, 6\}, \\ &\boldsymbol{\tau}_{\text{wave2}} = \begin{bmatrix} d_1 & d_2 & d_6 \end{bmatrix}^T. \end{aligned} \tag{9}$$

Finally, the ocean current speed is modeled as $V_c = \bar{V}_c + V_{\text{GMc}}$. V_{GMc} is mean current speed, and V_{GMc} is noise from generating a first-order Gauss–Markov process

$$\dot{V}_{\text{GMc}} + \mu V_{\text{GM}} c = w, \tag{10}$$

where w is Gaussian white noise and $\mu \geq 0$ is a constant. The direction of the current is typically given by a constant current angle α_{V_c}. Furthermore, the current speed is usually limited using a saturating element based on the maximum reasonable current speed.

2.3 DP control

The DP models are typically only valid for maneuvering up to approximately 2 m/s due to quadratic damping becoming significant at this speed. However, as docking is typically performed in low-speed regions, a DP control system is considered appropriate for the docking method.

A multiple-input and multiple-output (MIMO) PID controller is a typical starting point for a DP system. The desired control force $\boldsymbol{\tau}$, given the error $\tilde{\boldsymbol{\eta}}$ between the pose $\boldsymbol{\eta}$ and the desired pose $\boldsymbol{\eta_d}$, is defined as

$$\boldsymbol{\tau} = -\boldsymbol{K}_p\tilde{\boldsymbol{\eta}} - \boldsymbol{K}_i \int_0^t \tilde{\boldsymbol{\eta}}(\tau)d\tau - \boldsymbol{K}_d\dot{\tilde{\boldsymbol{\eta}}}, \tag{11}$$

where the controller gains $\boldsymbol{K} = [\boldsymbol{K}_p, \boldsymbol{K}_i, \boldsymbol{K}_d]^\top$ are tuned based on the desired behavior of the controller. Here $\boldsymbol{\tau}$ is only a *desired* force, which must be feasible. The physical realization of the control force depends on the control allocation method, thrusters, and steering gear on the vessel. Delay and physical limitations such as input amplitude and rate saturations will impact how accurately the desired force is realized physically on the vessel.

2.4 Guidance and reference model

The control references for the DP control system are typically given by a *setpoint regulation* guidance system. The aim of this system is to close the distance between the vessel and static waypoints, by using a third order reference model for the desired pose $\boldsymbol{\eta}_d$, which filters each step in the input commands $\boldsymbol{r}^n$. By adding a time constant $T_i = 1/\omega_{n_i} > 0$, the reference model can be written as the transfer function of a low-pass (LP) filter [9, Chapter 11]

$$\frac{n_{d_i}}{r_i^n}(s) = \frac{\omega_{n_i}^3}{s^3 + (2\zeta + 1)\omega_{n_i}s^2 + (2\zeta + 1)\omega_{n_i}^2 s + \omega_{n_i}^3}, \tag{12}$$

which generalizes to multi-variable systems as

$$\boldsymbol{\eta}_d^{(3)} + (2\boldsymbol{\Delta} + \boldsymbol{I}_n)\boldsymbol{\Omega}\ddot{\boldsymbol{\eta}}_d + (2\boldsymbol{\Delta} + \boldsymbol{I}_n)\boldsymbol{\Omega}^2\dot{\boldsymbol{\eta}}_d + \boldsymbol{\Omega}^3\boldsymbol{\eta}_d = \boldsymbol{\Omega}^3\boldsymbol{r}^n. \tag{13}$$

$\boldsymbol{\Delta} > 0$ and $\boldsymbol{\Omega} > 0$ are diagonal design matrices for relative damping ratios and natural frequencies, respectively. They can be tuned to comply with the controller bandwidth to create achievable references for the physical system. The step command $\boldsymbol{r}^n$ gives smooth steps in $\boldsymbol{\eta}_d^{(3)}$ while $\ddot{\boldsymbol{\eta}}_d$, $\dot{\boldsymbol{\eta}}_d$ and $\boldsymbol{\eta}_d$ are low-pass filtered, which gives a smooth reference signal for the setpoint tracking control system.

3 Automatic docking with dynamic positioning

The proposed docking method is divided into three phases, each with different control strategies, using only pose data from a dual antenna Global Navigation Satellite System (GNSS) as state measurements. The phases are defined as

1. Approach phase: Approaching the berthing area using position control through dynamic positioning, and aligning the vessel heading with the quay structure.

2. Berthing phase: Closing the distance to the quay structure with velocity control while maintaining the desired heading using a modified DP controller.
3. Quay phase: Push the vessel towards the quay using a constant force in the direction of the dock, and sideways positioning and heading control to avoid slipping due to disturbances.

Fig. 2 illustrates the docking steps during normal operation. The architecture for the proposed DP control system for docking is illustrated in Fig. 3.

3.1 Approach phase

The purpose of the approach phase is to maneuver through the harbor area at a safe speed, and align the vessel for straight-line docking near the quay. The DP PID controller from (11) is utilized, with increased weight on keeping the desired velocity and heading, and less weight on position. It is deemed more important that the vessel align with the quay at a slow speed, than that the position of the vessel aligns exactly with the reference. Specifically, the controller gains are greater in the yaw direction than surge and sway, and greater for the damping control than the proportional and integral control. The gains are typically defined as

$$\begin{aligned} \boldsymbol{K}_p &= diag\left(K_{p1}, K_{p1}, K_{p2}\right), \quad K_{p1} < K_{p2}, \\ \boldsymbol{K}_i &= diag\left(K_{i1}, K_{i1}, K_{i2}\right), \quad K_{i1} < K_{i2}, \\ \boldsymbol{K}_d &= diag\left(K_{d1}, K_{d1}, K_{d2}\right), \quad K_{d1} < K_{d2}, \\ \boldsymbol{K}_d &> \boldsymbol{K}_p, \boldsymbol{K}_i \ , \end{aligned} \tag{14}$$

and must be tuned to fit the chosen vessel and actuator design, see Appendix A.

For comparison during testing and development purposes, the starting point WP1 is where the vessel initializes the approach phase with a specific pose and zero velocity.

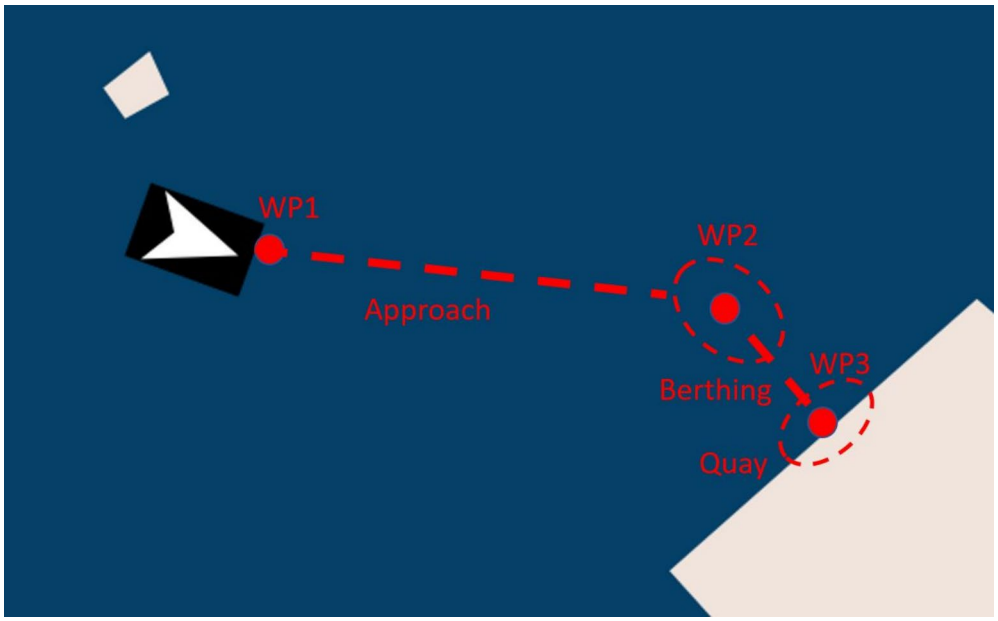

Fig. 2 Proposed docking procedure

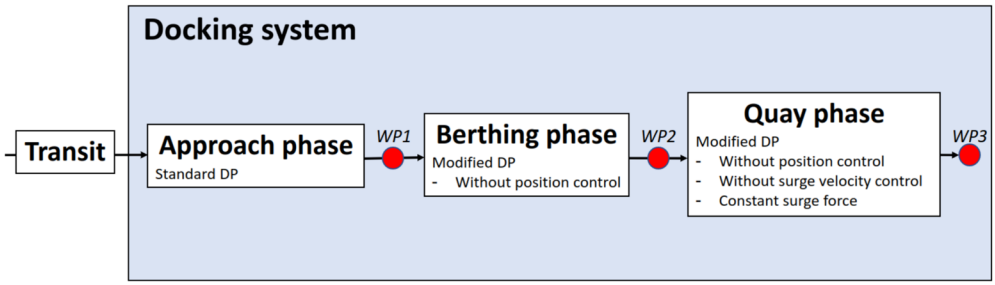

Fig. 3 Docking control system using modified DP, with transitions at waypoints between phases

In accordance with the flexibility of the proposed docking method, it can be chosen anywhere in the quay area, within reasonable and obstacle-free distance to the quay structure. In regular operation, the vessel would enter this waypoint with speed from the previous transit phase. From field testing, this is assumed to have little practical difference when entering the approach phase at low speed.

The transition from a more high-velocity transit phase to the low-velocity berthing phase might benefit from a bumpless transfer control scheme [26]. Bumpless transfer might also improve the docking procedure during the transitions between each phase, if controller changes cause undesirable bumps in the control input during docking.

3.2 Berthing phase

During berthing, it is important to ensure a low velocity to avoid hard collision with the quay, and to align the heading with the quay to enable stable contact. Therefore, WP2 should manually be set directly in front of the quay structure, within a few meters depending on the vessel and quay size. The proposed solution is then to disable position control both in surge and sway during this phase, to avoid sudden accelerations and dependence on very precise GNSS data, when moving slowly towards the quay.

The proposed PID controller structure only keeps control in velocity and heading, and can be applied in both longitudinal and lateral direction of the vessel. For longitudinal docking, in surge direction, head on the quay, the references are a low desired surge velocity reference $\boldsymbol{\nu}^b_{\text{ref}}$ and zero desired sway velocity reference:

$$\boldsymbol{\nu}^b_{\text{ref}} = \left[u_{\text{ref}}, 0, 0\right]^\top. \tag{15}$$

This is enabled by modifying the DP controller gains $\mathbf{K}$ from (11) such that the control force only depends on the heading and velocity. The controller gains for the berthing phase become

$$\begin{aligned} \boldsymbol{K}_p = diag\left(K_{p1}, K_{p1}, K_{p2}\right) &\rightarrow \boldsymbol{K}_p = diag(0, 0, K_{p2}), \\ \boldsymbol{K}_i = diag\left(K_{i1}, K_{i1}, K_{i2}\right) &\rightarrow \boldsymbol{K}_i = diag\left(0, 0, K_{i2}\right), \\ \boldsymbol{K}_d = diag\left(K_{d1}, K_{d1}, K_{d2}\right) &\rightarrow \boldsymbol{K}_d = diag\left(K_{d1}, K_{d1}, K_{d2}\right). \end{aligned} \tag{16}$$

Similarly, the gains and references can be set for lateral docking, in sway direction, with the heading parallel to the quay, with a low desired sway velocity reference and zero desired surge velocity reference. However, only the control, guidance and result from longitudinal docking will be presented in this article.

During this phase, the reference filter (13) is turned off, which might initiate a bump in reference during the switch, however this issue is addressed in Sect. 3.4. Thus, $\boldsymbol{\nu}^b_{\text{ref}}$ is the only reference signal given to the controller, along with the desired heading angle given by the quay angle α_{quay}. This enables a slow and steady speed towards the final quay phase. The desired, allowable velocity range u_{quay} when making contact with the quay depends on the dynamics and robustness of the vessel front and quay structure, like if there are fenders or tires protecting the surfaces.

3.3 Quay phase

The quay phase aims to maintain contact between the vessel and the quay. Thus, WP3 should be set at the tip of the quay structure. The chosen control structure is based on a constant force in the direction of the quay, which for docking in surge direction is $\boldsymbol{\tau} = [k, 0, 0]^\top$. Here, k is a tuneable control force dependent on the vessel, the quay structure and environmental forces, see Appendix A for tuning. This simple controller structure does not consider the vessel state, so an important assumption is that the vessel already has the desired pose next to the quay when entering this phase. Since the quay may be floating and moving, a constant force will give a stable contact, unlike a position or velocity controller that would require modifications in that case.

Varying environmental forces may become a significant challenge for this phase, as the vessel is no longer able to keep control of the heading without any sideways force. Consequently, a method for sideways control is proposed to supplement the constant force with the control forces from the berthing phase in the other two DOFs. For docking head-on with zero velocity in sway and yaw, this is implemented by maintaining both the controller gains from the previous berthing phase in yaw direction, and the damping control in sway. Thus, the desired control force $\boldsymbol{\tau}$ in the quay phase is

$$\boldsymbol{\tau} = \begin{bmatrix} k \\ 0 \\ 0 \end{bmatrix} + \boldsymbol{\tau}_{\text{pid}}. \tag{17}$$

As the vessel has reached its goal and no longer follows a reference pose from the guidance system, the references for $\boldsymbol{\tau}_{\text{pid}}$, Eq. (11), are set to the last references from the berthing phase. This strategy is viable when assuming the vessel had the correct pose when entering the quay phase, since the new desired pose of sway and heading would be the same as in the end of the berthing phase. Also, it assumes the size of the quay is larger than the width of the vessel by a safety margin. The specific size of this margin depends on the vessel size and physical constraints of the docking area.

3.4 Phase transitions

For smooth transitions between the different docking phases, the idea is to switch to a new phase when entering an ellipse of acceptance around the waypoints. Each waypoint consists of a position $[x^n, y^n]^T$ and a desired heading angle α_{WP}.

As the classical DP controller attempts to close the distance between the vessels center of origin (CO) and the waypoint, the vessel will eventually slow down before reaching the waypoint in the approach phase. However, this is undesirable, since the vessel must then reaccelerate when maneuvering towards the next waypoint. With the proposed transition ellipses around the waypoints, the vessel avoids stopping at each waypoint, by moving on as soon as the vessel enters the waypoint ellipse. The ellipses are created with center in the waypoint and rotated with the desired heading angle α_{WP}, and can be seen in Fig. 2. Thus, the area of acceptance becomes the area within the ellipse around the waypoint, with center $[x_c^n, y_c^n]$, and the formula for deciding if the CO of the vessel is within the ellipse is given as

$$\frac{\left(\left(y_c - y^n\right)\cos\left(\alpha_{WP}\right) - \left(x_c - x^n\right)\sin\left(\alpha_{\text{WP}}\right)\right)^2}{a^2} - \frac{\left(\left(y_c - y^n\right)\sin\left(\alpha_{\text{WP}}\right) + \left(x_c - x^n\right)\cos\left(\alpha_{WP}\right)\right)^2}{b^2} \leq 1. \tag{18}$$

The semi-major axis denoted by a and the semi-minor axis denoted by b give the shape of the ellipse. Typically, the ellipse at the quay should be short in the semi major axis, to ensure the simple controller in the quay phase is not activated too early. The length of the ellipse at the quay should also be within the physical limits of the quay, to avoid missing the quay and causing dangerous situations. Using lines for transitions is another viable strategy that can be considered in open ports with more space.

The angle α_{WP} is used as a second requirement for the transition at the waypoints, where the heading ψ of the vessel must be within a range $[\alpha_{\text{WP}} - \alpha\,^\circ, \alpha_{\text{WP}} + \alpha^\circ]$. Here, α should be chosen low enough to ensure a reasonable heading angle when transitioning to a new docking phase based on the geometry of the quay and the yaw stability of the vessel. When the final two waypoints are aligned normally to the quay, α_{WP} is set equal to α_{quay} to keep the vessel heading straight on for the berthing and quay phases.

3.5 Time-efficient docking

The efficiency of the proposed docking method compared to manual operation is a critical consideration. One can also argue that an important part of time efficiency is to dock successfully on the first attempt, as manual docking may require several attempts due to human errors and the general challenges of the docking task.

The duration of the method depends on the vessel and quay area, the waypoint placement and heading range, the reference model and the tuning of the control system. The proposed strategy is to tune the reference velocities and transition ellipses, two critical parts of the docking method. This approach will not provide an optimal solution for time efficiency, but an improvement compared to a constant low-velocity reference, and enable the method to achieve a similar performance as a manual docking maneuver. This solution will also be faster than docking with pure DP control, which only controls speed indirectly and are thus unable to precisely maintain a desired speed without highly accurate positioning and use of waypoints.

This design is also meant to increase the modularity of the proposed docking method, as it does not include complicated optimization constraints or complex real-time computations.

To increase the forward speed in the berthing phase, the reference velocity in surge can be implemented as a downwards step function, exemplified in Fig. 4. This allows higher speeds in the beginning of the phase, while still reaching the desired low speed before the quay phase. The magnitude and timing of the step velocity u_{ref} must be tuned, based on the vessel and the distance to the quay structure from WP2, see Appendix A for a tuning approach.

Additionally, the transition ellipse between the approach and berthing phase can be tuned to maintain the forward velocity during transition. Increasing the ellipse of acceptance around WP2 and the heading acceptance range will allow the vessel to initiate the berthing phase earlier, and as such avoid any unnecessary deceleration close to the waypoint. However, the vessel must not transition too far away, or with a large error in heading, as the reduced PID controller in the berthing phase may struggle to complete the docking. See Appendix A for a tuning approach.

4 Challenging environmental conditions capability

The proposed docking algorithm can be improved by knowing the vessel's capabilities to handle environmental forces acting on the vessel during docking. This section describes how to analyze the capability of the docking system for a vessel, and how the control system can be adjusted during challenging environmental conditions.

4.1 Docking capability

From an industrial point of view, the docking system should be aware of its own capabilities to assess if a successful automatic docking is possible in the conditions present. The DP

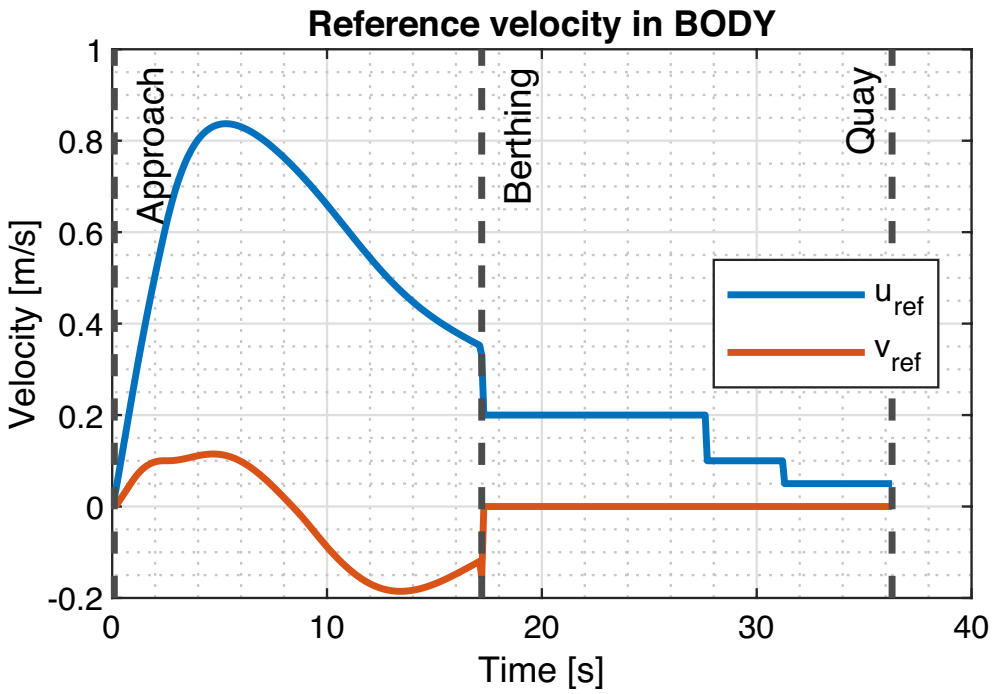

Fig. 4 Proposed tuned reference velocities

dynamic capability analysis [23] is useful to determine the station-keeping capabilities of a vessel. For the automatic docking method, the analysis can be extended to determine the capabilities of following the reference trajectory during the docking process. A straightforward approach is to find the mean environmental forces that will prevent the vessel from reaching the desired waypoint during each phase, and use that as criteria to activate alternative strategies.

The acceptance criteria for finishing each phase can be defined as staying on the inside of certain channel boundaries around the waypoints, see Fig. 5. From systematic testing using a simulator with different combinations of speed and direction of environmental forces, capability plots for the docking phases can be created. If the docking system observes environmental forces greater than the capabilities of one of the docking phases, other strategies should be considered to complete the docking safely and in time. For simplicity, only criteria based on wind forces are shown in this article, however a combination of all types of environmental forces would also be reasonable. In the capability plot in Fig. 5, the outer numbers are wind direction angles relative to the vessel, the inner numbers are wind speeds, the black border is the limit based on the acceptance channels, the dark blue area is when the disturbances significantly increase the docking duration and the vessel almost exceeds the acceptance channels, and the light blue field is within the capability of normal operation.

4.2 Increased integrator force for improved docking performance

One potential use of the capability analysis is to assess observations of the environmental conditions before making decisions, to enable docking under challenging conditions. If the docking system is functioning normally, and the environmental forces acting on the vessel are estimated to exceed the docking capabilities, alternative strategies can be activated based on the estimated direction and magnitude of the environmental forces. This could be by modifying the control force, waypoints or the controller reference signals for the vessel. Here, one specific strategy for modifying the integrator force of the DP control system will be investigated as showcase, with results in Sect. 6. Moreover, other potential strategies for improved docking in challenging conditions are discussed later in the same section.

The proposed strategy is to modify the gain $\boldsymbol{K}_i$ of the integrator in the PID controller (11). The integrator typically mitigates effects from slowly varying environmental forces constantly pushing the vessel in a specific direction. Usually, the integral term is saturated by an anti-windup scheme, to avoid critical control actions if the accumulated error increases without a bound. However, due to the transitions between phases, the control system can go from a saturated state before a transition to a non-saturated state after a transition. Consequently, increasing $\boldsymbol{K}_i$ can be an effective

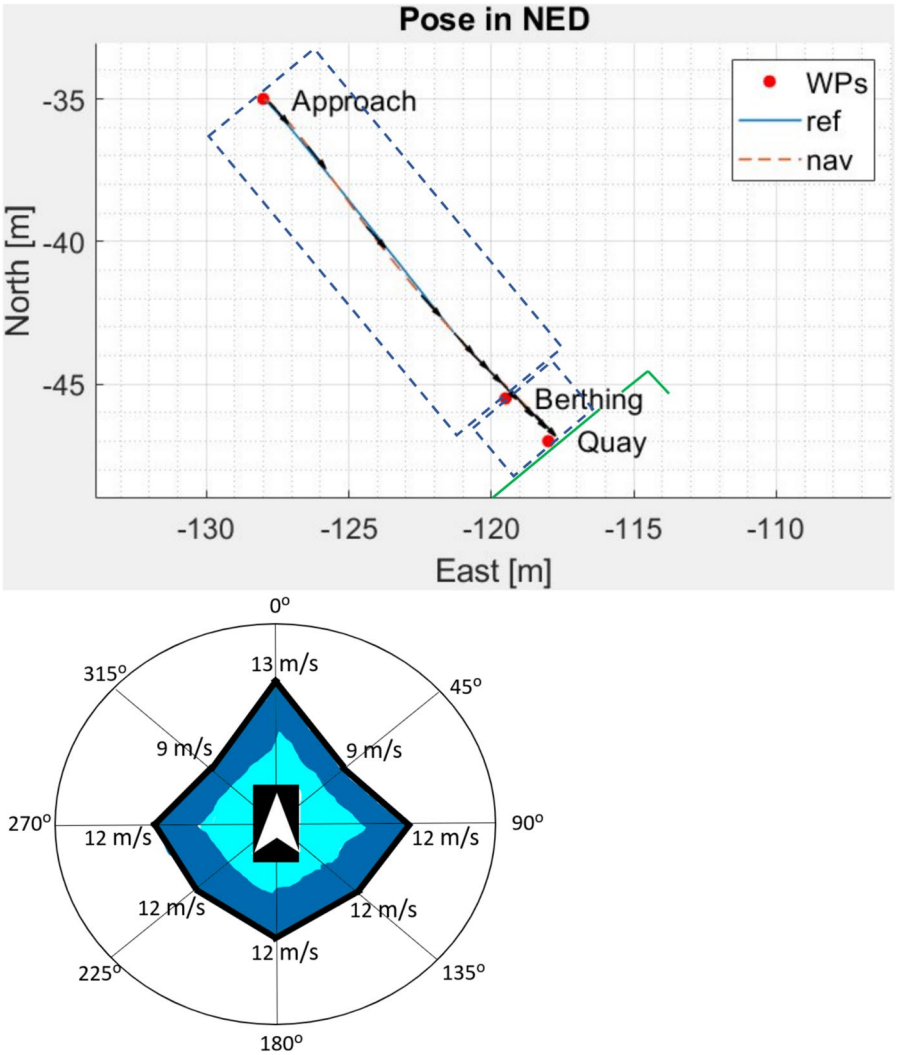

Fig. 5 Acceptance criteria channels (top) and example of docking capability plot (bottom). The waypoints *WPs* are red dots, the acceptance channels are dashed blue lines, the quay is marked with green lines, the vessel heading is marked by the black arrows, and the reference position *ref* and the position measurements *nav* are the blue and dashed orange lines, respectively

strategy to allow for more thrust from the control system immediately after phase transitions.

If the estimated environmental forces exceed the docking capabilities, increasing the limit of $\boldsymbol{K}_i$ can also enable more control force relative to the other PID terms, to better counter the accumulated error caused by the disturbances. This will allow more of the vessel's available control force to counter the environmental disturbances pushing the vessel out of the docking channels. Especially, during phase transitions, when the change of references might otherwise cause a significant reduction of the control forces acting towards the disturbances, the increased desired integrator force from previous accumulated errors may be helpful to keep the vessel on track to complete docking.

5 Experimental setup

The testing platforms are a simulator and a physical ferry named *milliAmpere* [27]. The milliAmpere ferry and its waterline footprint are illustrated in Fig. 6. The ferry is a fully actuated and controllable system in 3 DOF, enabled by two rotatable azimuth thrusters using a nonlinear scalar control allocation [28]. The sensor system for measuring position and heading is a Vector^{TM} VS330 GNSS receiver with dual antennas. The small ferry is designed similar to a typical car or passenger ferry, for docking with the bow or stern against the quay structure, and with a ramp that moves down for easy embarking and disembarking.

The simulator contains a 3 DOF vessel model of the physical milliAmpere ferry, and also includes models for environmental forces and a static quay structure. The vessel and environmental forces are modeled as described in Sect. 2, while the quay structure follows a mass-spring-damper model with added Coulomb friction forces, to simulate the

Fig. 6 The milliAmpere ferry (top) and its waterline footprint (bottom)

bounce and friction of fenders or dampers at the quay. For simulating the vessel behavior with the maneuvering model, the differential equations are solved using a Runge–Kutta 4th order (RK4) method.

6 Results and discussion

This chapter presents the results obtained from the testing platform, and discussions of the results and methods proposed in this article. First, the results from simulator and field testing of the automatic docking method are presented, followed by docking capability analysis and the strategy to counter challenging disturbances.

6.1 Automatic docking method

The results are obtained from testing in the simulator, as well as experimental field testing with the milliAmpere ferry in Havnebassenget, Trondheim, on November 3rd 2021. For better comparison, the docking sequences in the simulator and field were designed as equal as possible. They both have the same start position WP1 with a sideways angle $\alpha_{start} = 120°$, and attempts to dock longitudinally, head-on at the quay, at an angle $\alpha_{quay} = 137.95°$, as illustrated in Fig. 2. While WP1 is set rather arbitrarily within collision-free distance to the quay, WP2 is aligned directly in front of the quay, and WP3 is placed at the tip of the quay structure. Based on observations from previous field tests, a realistic set of environmental disturbances in the simulator was chosen as a combination of 6 m/s wind and 0.4 m/s ocean current forces in the North-East direction. In the pose figures, the heading is illustrated as black arrows.

Figures 7 and 8 illustrate the pose and velocity, respectively, of a docking procedure in the simulator. Docking was completed in 36 s. Figures 9 and 10 illustrate the pose and velocity, respectively, of a docking procedure in field trials. Docking was completed in 37 s in the field experiment.

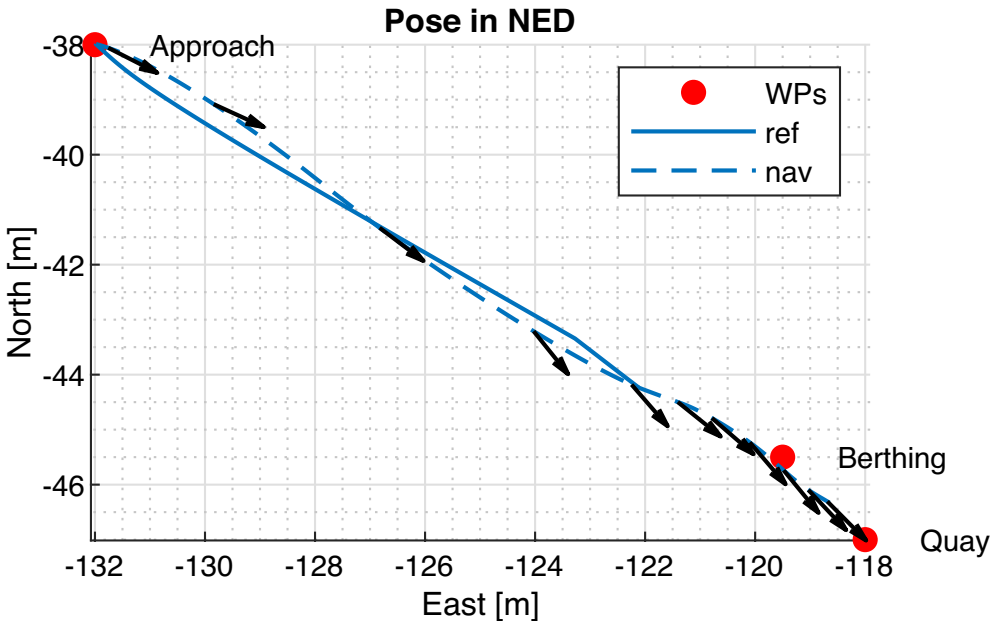

Fig. 7 Pose in NED from docking in simulator

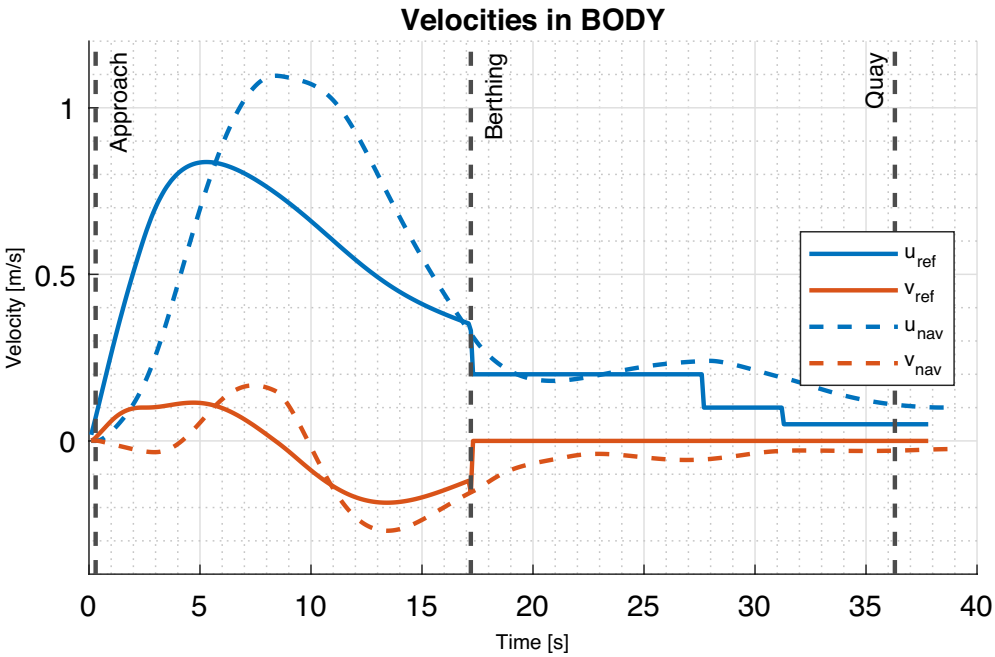

Fig. 8 Velocities in BODY from docking in simulator

From the figures of vessel pose during docking, it is apparent from the measurements *nav* that the vessel is not able to follow the reference *ref* points initially. This is due to the transients of the integrator that needs time to build up, to counter the environmental forces acting on the vessel. However, the vessel manages to converge towards the waypoints and make contact with the quay in the end, see Fig. 11, with about 1 m deviation.

The deviation from the berthing and quay waypoints are accepted by the proposed waypoint ellipses, which allows the vessel to complete docking without stopping at each waypoint. Specifically, the pose plot from Fig. 9 illustrates

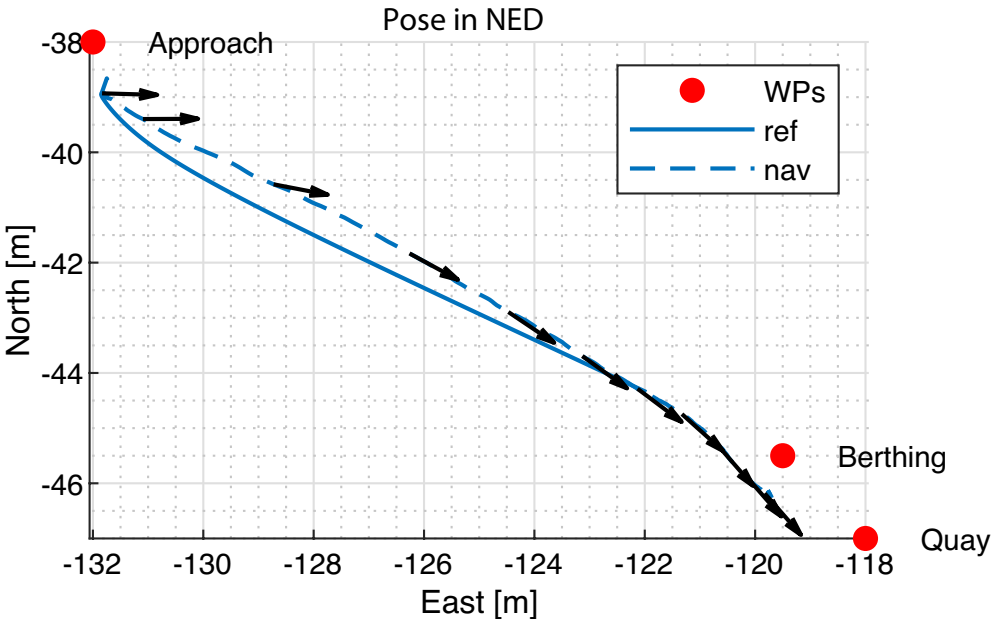

Fig. 9 Pose in NED from docking in the field experiment

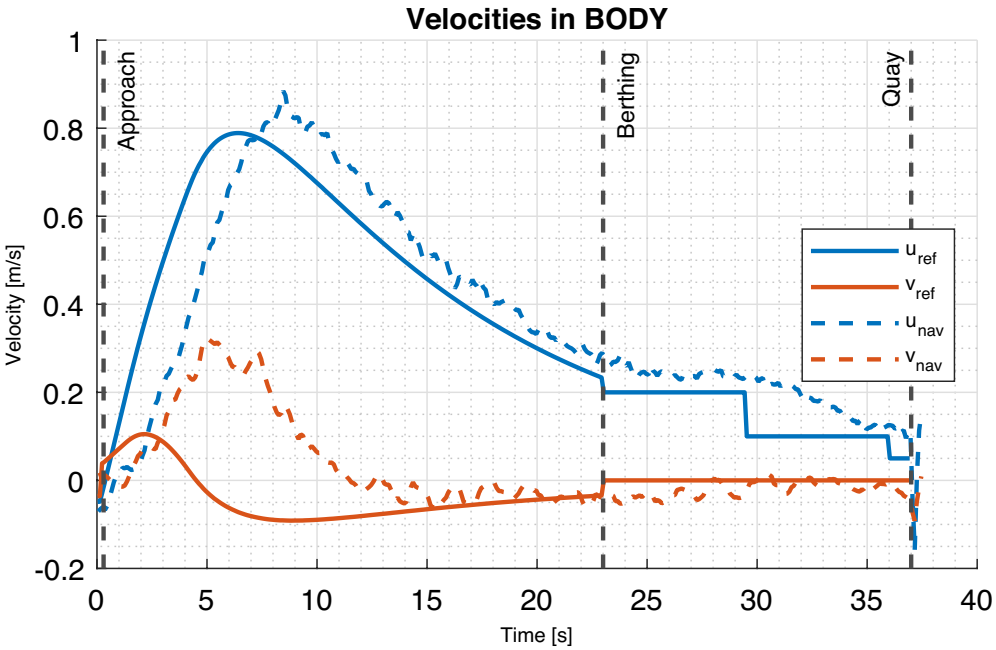

Fig. 10 Velocities in BODY from docking in the field experiment.

how the waypoint ellipses enable the vessel to transition and dock without moving directly through the waypoints, Here, the size of the final quay ellipse must still be within the physical constraints of the quay structure. During testing, it was seen that too small ellipses would slow down the vessel unnecessarily, while too large would risk the vessel to drift sideways and not complete the last docking phases within the acceptance criteria.

The low-level controllers could be tuned more accurately for the DP system in these experiments. However, following the idea of a scalable docking system for existing DP systems, the performance of the DP system is not considered as the main focus here.

Fig. 11 Vessel pose before contact with quay structure during docking in Havnebassenget

The black arrows in Figures 7 and 9 illustrate the vessel heading. The vessel rotates slightly while it approaches the waypoints, both during testing in simulator and field. However, it is sufficiently head-on when making contact with the quay to stay stable with the front pushed against the quay, without rotating and colliding with one of it's sides. Moreover, from observations and experience, the accelerations during the docking process are small enough to avoid causing discomfort for any passengers.

The illustrations of the velocity in Figures 8 and 10 indicate that while the vessel does not track the desired velocity perfectly, it still manages to reach each waypoint and slow down before making contact with the quay. The main deviations are from the integrator transients, the environmental disturbances, and tuning of control system and reference model. Testing found that the suitable final velocity range for milliAmpere and this quay structure was $u_{\text{quay}} = [0, 0.5]$ m/s, to avoid a big impact causing drift, or discomfort for passengers.

It is important to note that for all the tests in this article, the vessel starts at rest in WP1, and must accelerate during the approach phase. During normal operations however, the vessel should enter WP1 at transit speed, ideally below 2 m/s for the validity of the DP model, from the previous transit phase using a different controller than DP. Thus, the vessel would use the approach phase to decelerate towards WP2, and a bumpless transfer scheme between the controllers would be necessary to avoid critical bumps in control during the transition from transit to docking [26, 29, 30].

Another consideration is the behavior during the quay phase. Given the assumptions in this article, the task is to make soft contact with the quay, and then stay connected. This creates high demand for the precision of the speed and the control force to keep the vessel at rest.

For comparison of the docking results in simulator and field tests, the most noticeable differences are regarding measurement data and the obtained speed. As seen in Figures 9 and 10, the method is capable of automatic docking with the milliAmpere ferry during typically calm conditions. The velocity from the measurements, u_{nav} and v_{nav}, are noisy due to the uncertainty in the GNSS sensor and the low sampling rate, but this does not seem to impact the method.

When comparing the velocity in the field test with the velocity in the simulator in Fig. 8, it is apparent that the vessel is slower to react and accelerate in the field test than in the simulator. This delay is probably caused by modeling errors in the simulator. However, the vessel is still able to reach a low speed before making contact with the quay within a very similar time, and then stay connected. Due to the noisy measurements and the dynamics of the tires at the quay structure, it appears as the vessel in the field test has a sudden fluctuation in the velocity, while in reality it was kept still, pressed towards the tires, with a slight bounce.

Note, in Fig. 9 that the front of the vessel makes contact with the quay, even though the motion of the center of origin ends about one meter away from the quay waypoint. This is due to the shape of the vessel, as the front of the vessel makes contact with the quay at this point, which must be considered when tuning the quay ellipses.

6.2 Capability and docking under challenging conditions

Additional results from docking capability analysis and comparisons of strategies for improved docking in this section

are obtained from testing in the simulator, due to the lack of ground truth in the field. The applied environmental forces are modeled as in Section 2.2.

6.2.1 Docking capability

Figures 12, 13 and 14 illustrate the capability of the longitudinal docking procedure during slowly varying environmental disturbances from wind forces. The plots are based on obtained values for wind speeds from testing with straight-line docking. The acceptance channel for the approach phase is about five times the width of the milliAmpere vessel, while they are about three times the width for the berthing and quay phases. The capability plots clearly illustrate that the capabilities vary with the direction of the wind, as expected. These results are consistent with the operative experience from both simulator and field tests conducted with the milliAmpere ferry.

For the approach phase, the milliAmpere vessel in the simulator is able to reach WP2 when influenced by wind with speed of 12 m/s from most angles. Although wind speeds at 10 m/s are not considered extreme, they are still significant with respect to the size and thruster effect of the milliAmpere ferry, and deemed to be abnormal conditions in Havnebassenget. It is also considered a strong wind by others [24], and stronger wind conditions would require an improved propulsion system. The worse capability for disturbance from 45° and 315° seems to be due to the heading control and tuning, which here focuses too much on keeping a straight heading, and fails to also follow the position reference and stay within the channels. As expected, the berthing and quay phase are most resistant to disturbances along the x_b axis, straight on the quay.

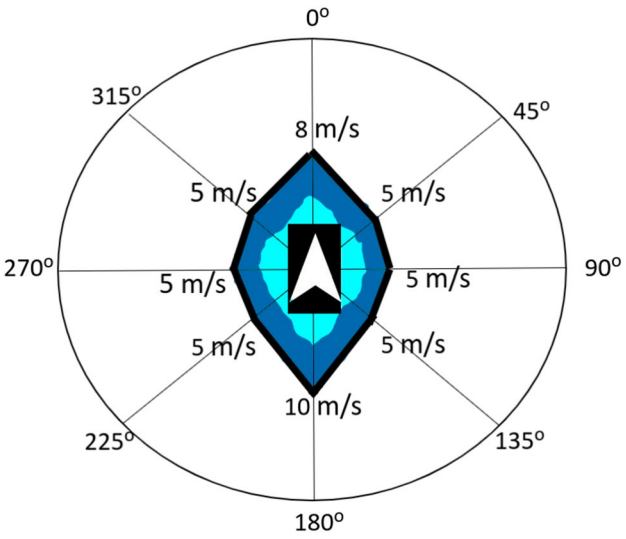

Fig. 13 Docking capability plot for berthing phase

The capabilities are reduced for each phase. Especially with sideways wind pushing the vessel out of the channels, the berthing and quay phase controllers show significantly worse performance than the approach phase controller. This is expected, because of the chosen control structure in the last two phases, which do not consider state errors in position, but only in velocity and heading. Moreover, as described previously, the acceptance criteria channels are smaller for the last phases. For the quay phase, it is deemed less important with high capabilities, as the vessel should be assisted by hatch mechanisms, and friction from the tires or fenders at the quay. These features are not available in the simulator.

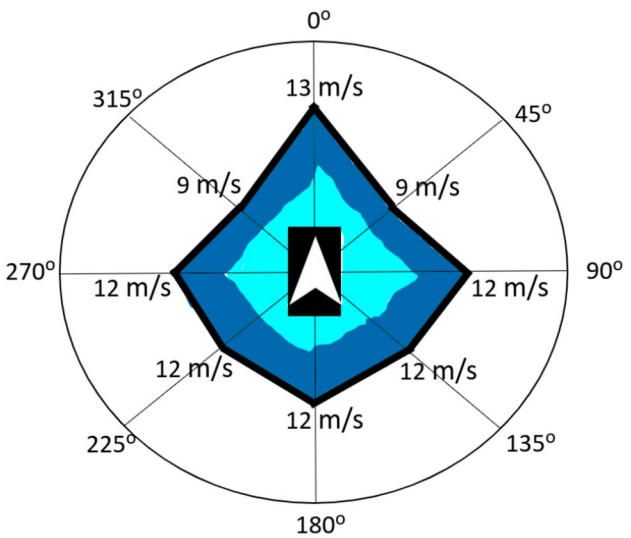

Fig. 12 Docking capability plot for approach phase

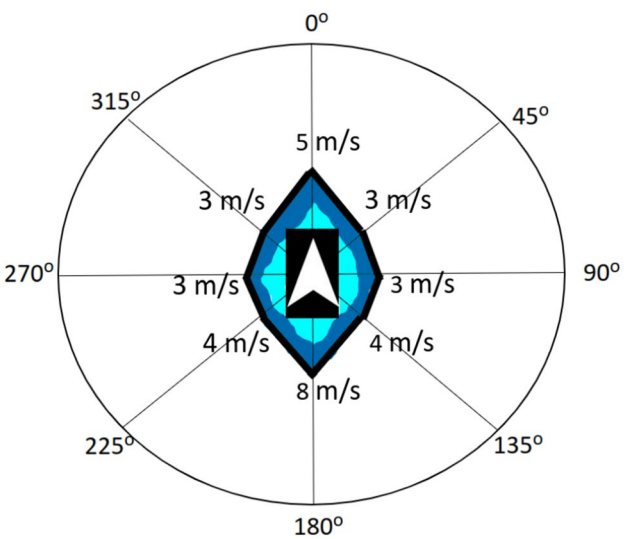

Fig. 14 Docking capability plot for quay phase

The berthing phase capability could be improved, even with smaller acceptance channels, as the wind speeds lie within a range of 2–6 m/s during normal conditions in Havnebassenget. This motivates the need for improved control from alternative strategies, to complete docking when exposed to typical yet challenging conditions. A better tuned system may also have a better and more responsive heading controller to counteract the disturbances.

Some simplifications were made during this analysis, as testing was only done with longitudinal, straight-line docking. The capability analysis could include docking from a sideways encounter angle, to determine the capabilities when turning the vessel during each phase. This calculated capability is expected to be a little lower due to the maneuvering model with a decoupling of surge and the focus on heading control.

Setting the acceptance criteria as channel boundaries, compared to a circle around a station-keeping point in the original DP capability analysis, seems to be a useful approach for docking. This way, the docking capability analysis determines the capability of the DP controller to stay within a larger station-keeping rectangle during straight-line docking, with velocity within the valid range for DP. From the results in the simulator, there are no inconsistency with this increased acceptance limit, as the vessel will consistently fail or succeed to dock based on the presented limits for wind disturbance. Other types of disturbances could also be included during the analysis to further validate the resulting capabilities.

6.2.2 Strategies for improved docking performance

The final simulation results showcase the increased integrator strategy that can be activated to counter strong environmental forces exceeding the docking capabilities. Finally, a discussion follows of how this strategy compares to other potential methods for improved docking performance. In the case presented, the simulated disturbance is a combination of wind with speed 8 m/s and ocean current with speed 0.4 m/s, both going in the North-East direction. For increased integrator force, the docking system has been active with the vessel at rest at WP1 for sufficient time for the integrator term to converge before starting docking.

Figures 15 and 16 illustrate a failed docking attempt and the strategy of increased integrator force, respectively. Figure 17 compares the desired control forces of the failed docking attempt with the desired control forces for the increased integrator strategy.

In Fig. 15, for the benchmark of this case of challenging conditions, a failed attempt of the regular docking procedure is illustrated. Due to the strong sideways wind and ocean currents exceeding the docking capabilities in the berthing phase, the vessel is pushed out of bounds and fails to reach the waypoint at the quay structure. Meanwhile, the method of increased integrator force relative to the other PID forces,

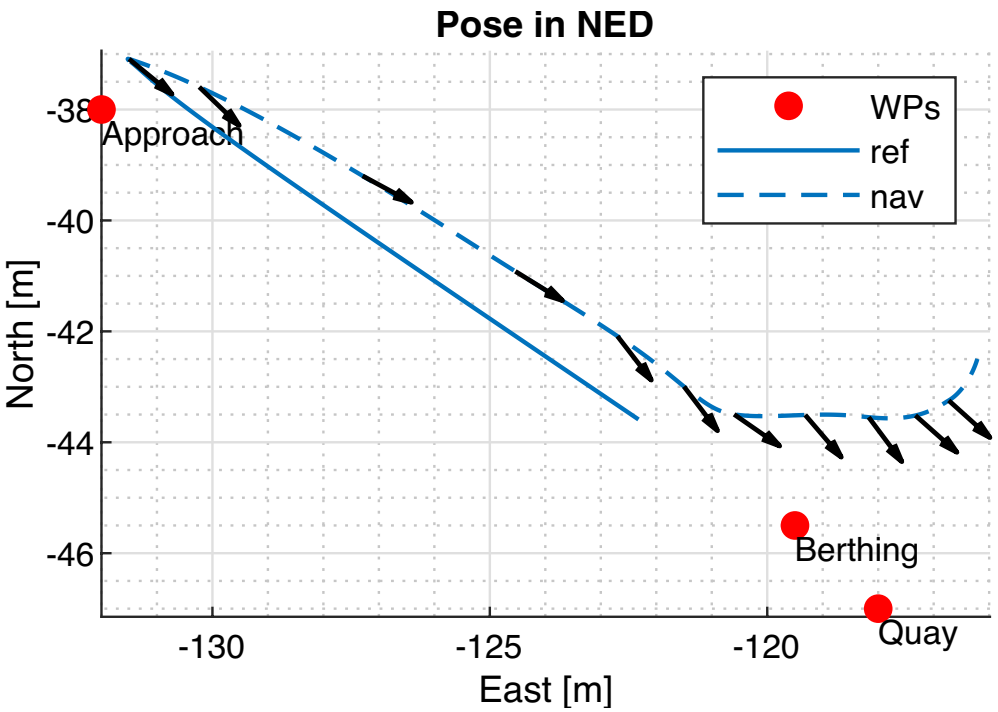

Fig. 15 Pose in NED from failed docking attempt due to strong wind towards North-East

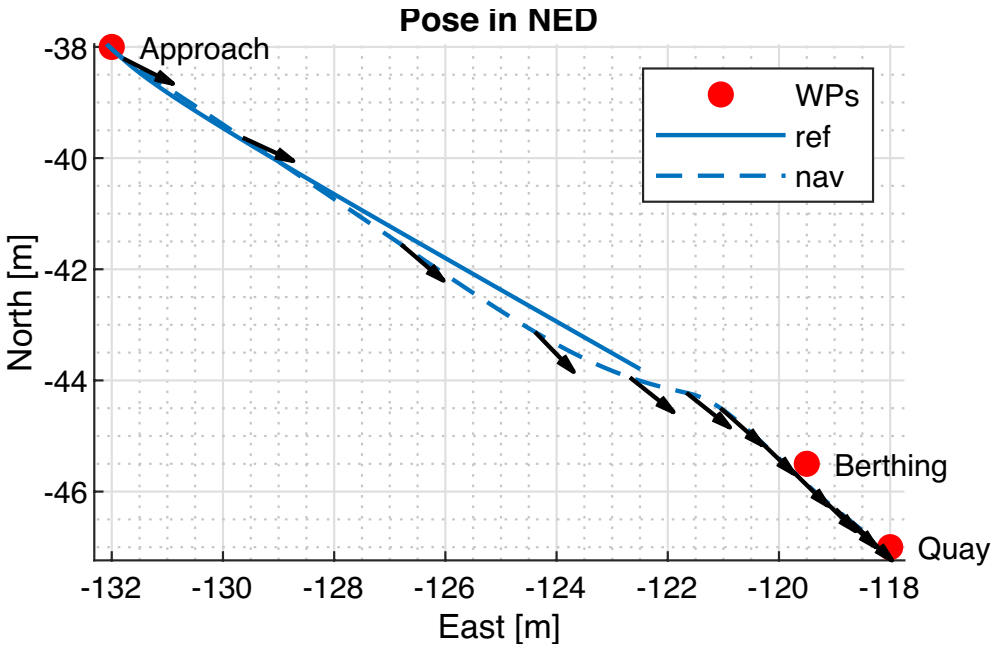

Fig. 16 Pose in NED with strategy of increased integrator force, with strong wind towards North-East

Fig. 17 Comparison of thrust in NED from failed docking attempt and from increased integrator strategy

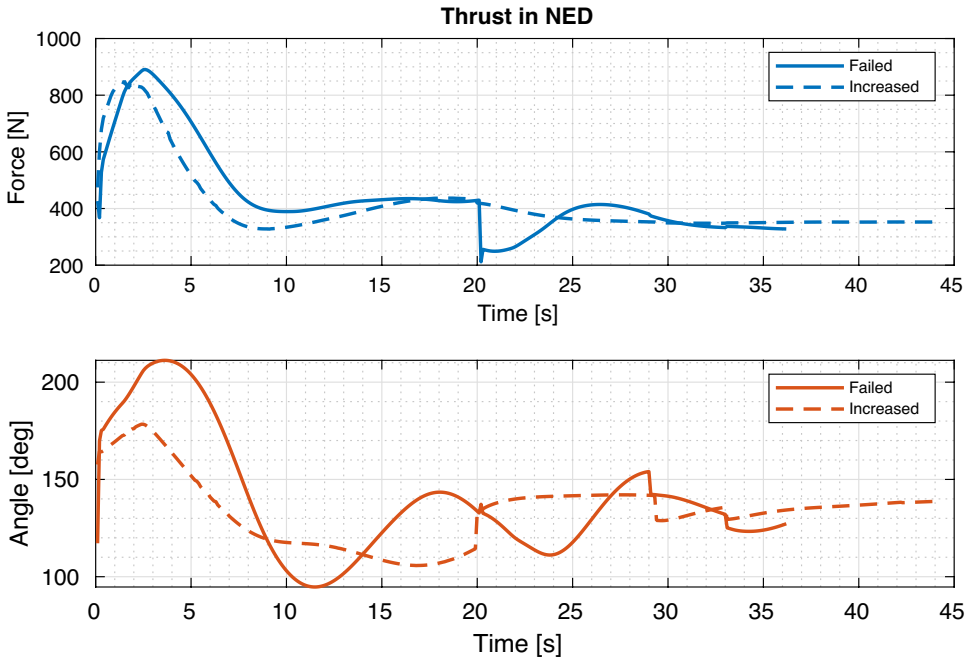

illustrated in Fig. 16, manages to safely complete docking in the same conditions. One of the reasons for why it improves on the regular method is due to the increased applied force, given by the integrator term, in the South direction for the first two seconds of docking, against the disturbances. Later, the desired force is more stable as it follows the reference, and during the transition to berthing phase the integrator force remains high enough to withstand the disturbances, whereas the desired force in the original method drops due to the relative impact of the change of reference on the PID terms. This showcases the usefulness of additional methods to be activated when the vessel is exposed to challenging conditions.

During this work, other methods for improved docking under challenging conditions has also been tested in the simulator. One potential method is to add a bias term

representing environmental forces to the 3 DOF maneuvering model in (3b) and estimate the environmental forces in a Kalman Filter (KF) [31]. The estimated bias can then be used directly as a feedforward term to the desired control force, similar to wind feedforward for DP systems [9, 32]. This method also seems promising for direct mitigation of disturbances, but it relies on accurate bias estimates, which again relies on accurate system identification and tuning of the KF.

Another potential method is to restart the docking procedure with a new encounter angle. During harsh conditions of slowly varying wind or ocean current, it can be beneficial to change the vessel encounter angle to complete the approach. Typically, operators will change the vessel heading to mitigate the influence of environmental forces, based on the vessel shape and distance to the next waypoint. There are multiple approaches to determine the alternative positions of the new starting point WP1, and potentially also WP2. In this work, the alternative waypoints were determined manually beforehand, but they could also be chosen automatically based on the estimated environmental forces [33]. Others have looked at determining waypoints for safe path in congested waters to avoid collisions [34]. The docking algorithm proposed here is flexible and can be extended to include such functionality.

7 Conclusion and future work

This article presented an automatic docking method for small vessels influenced by time-varying environmental disturbances. The proposed method performs docking with a DP controller and a guidance system based on waypoints and transitions between phases. This automatic docking method is only considered partly autonomous, as the transitions between phases and reference velocity must be adjusted by an operator with knowledge of the vessel and docking area. However, all the sub-methods are scalable and can easily be extended by automatic path planning systems.

Experimental testing in simulator and field have provided satisfactory results regarding both efficiency and performance in challenging environmental conditions, as proof of concept for scalable and flexible automatic docking of a small passenger ferry.

Both the introduced docking capability and the proposed strategies should be analyzed with more types and combinations of environmental disturbances like wake waves and wind gusts. They should also be tested more comprehensive in field experiments with complex, challenging environmental conditions.

Appendix A. Models and tuning

For simulation purposes, the following values for the milliAmpere vessel where used. An identification of the maneuvering vessel model (3b) gave the numerical values [27]

$$\boldsymbol{M} = \begin{bmatrix} m_{11} & m_{12} & m_{13} \\ m_{21} & m_{22} & m_{23} \\ m_{31} & m_{32} & m_{33} \end{bmatrix} = \begin{bmatrix} 2390 & 0 & 0 \\ 0 & 2448 & 268.1 \\ 0 & -23.84 & 4862 \end{bmatrix}, \tag{19}$$

$$\boldsymbol{C}(\boldsymbol{\nu}) = \boldsymbol{C}_{RB}(\boldsymbol{\nu}) + \boldsymbol{C}_{A}(\boldsymbol{\nu}) = \begin{bmatrix} 0 & 0 & c_{13}(\boldsymbol{\nu}) \\ 0 & 0 & c_{23}(\boldsymbol{\nu}) \\ c_{31}(\boldsymbol{\nu}) & c_{32}(\boldsymbol{\nu}) & 0 \end{bmatrix}, \tag{20}$$

where

$$c_{13}(\boldsymbol{\nu}) = -m_{21}u - m_{22}v - m_{33}r, \tag{21a}$$

$$c_{23}(\boldsymbol{\nu}) = m_{11}u + m_{12}v + m_{13}r, \tag{21b}$$

$$c_{31}(\boldsymbol{\nu}) = -c_{13}(\boldsymbol{\nu}), \tag{21c}$$

$$c_{32}(\boldsymbol{\nu}) = -c_{23}(\boldsymbol{\nu}), \tag{21d}$$

and

$$\boldsymbol{D}(\boldsymbol{\nu}) = \begin{bmatrix} d_{11}(\boldsymbol{\nu}) & 0 & 0 \\ 0 & d_{22}(\boldsymbol{\nu}) & d_{23}(\boldsymbol{\nu}) \\ 0 & d_{32}(\boldsymbol{\nu}) & d_{33}(\boldsymbol{\nu}) \end{bmatrix}, \tag{22}$$

where

$$d_{11}(\boldsymbol{\nu}) = 106.6 + 21.39|u| + 37.43u^2, \tag{23a}$$

$$d_{22}(\boldsymbol{\nu}) = 29.44 + 172.9|v| + 1517|r| + 1.338v^2, \tag{23b}$$

$$d_{23}(\boldsymbol{\nu}) = -62.58 - 488.7|v| + 198.2|r|, \tag{23c}$$

$$d_{32}(\boldsymbol{\nu}) = -7.34 + 4.352|v| + 437.8|r|, \tag{23d}$$

$$d_{33}(\boldsymbol{\nu}) = 142.7 + 122|v| + 831.7|r|. \tag{23e}$$

Tuning of the PID controller (14) for the DP control system is similar to previous work [5], providing the numerical values

$$\begin{aligned} \boldsymbol{K}_p &= [200, 200, 800], \\ \boldsymbol{K}_i &= [10, 10, 15], \\ \boldsymbol{K}_d &= [700, 700, 1600], \end{aligned} \tag{24}$$

with the initial and increased anti-windup term, respectively

$$\begin{aligned} \boldsymbol{\tau}_{i_{\text{windup}}} &= [150, 150, 200], \\ \boldsymbol{\tau}_{i_{\text{windup-increased}}} &= [250, 250, 200]. \end{aligned} \tag{25}$$

For tuning in the simulator of the step velocity u_{ref} from (15) in the berthing phase, the timing of the steps was tuned based on the vessels distance to quay. The magnitude was tuned based on the exit-velocity from the approach phase and the desired velocity when making contact with the quay. The goal is to find a balance between fast docking and low impact with the quay structure, which should also be tuned and verified in field. The chosen triggers for down-steps were 11m and 7m from the quay, and the magnitude for each step were 0.2, 0.1 and 0.05 m/s, respectively.

The constant control force k from (17) for the quay phase have been tuned based on testing in simulator and field, to determine the necessary force to keep the vessel pushed to the quay during relatively challenging environmental conditions. Another aspect to consider is the potential damage to the vessel and quay structure if the thrust is too large. The numerical value for the milliAmpere vessel is $k = 25$ N.

For tuning in the simulator of the transition ellipse sizes from (18), the size, rotation and acceptance angle was tuned for fast docking with low impact to the quay. The first ellipse at WP2 was chosen as a circle with $a = 3$ m and $b = 3$ m, which allowed for a smooth transition from the approach phase to the berthing phase, without losing much velocity. The acceptable heading deviation α was set to 10°, for the same reasons. The second ellipse at WP3 was chosen narrow in longitudinal direction and wide in lateral direction of the quay, as described in Sect. 3.4, with values $a = 1$ m and $b = 5$ m. The width b could also be set according to even stricter quay limitations, but in this case, the quay structure was wide enough to allow such a wide ellipse. The acceptable heading deviation α for this ellipse was set as 4°, as this enabled the milliAmpere vessel to slowly align its front with the quay, without drifting away.

Acknowledgements This work was supported by the Research Council of Norway with project number 296630. It was also in part supported by the Research Council of Norway through the Centres of Excellence funding scheme, project number 223254. The authors are grateful for the cooperation with Maritime Robotics. The authors would also like to thank Simen Krantz Knudsen for significant contributions in the software development.

Funding Open access funding provided by NTNU Norwegian University of Science and Technology (incl St. Olavs Hospital - Trondheim University Hospital). Open access funding provided by NTNU Norwegian University of Science and Technology (incl St. Olavs Hospital—Trondheim University Hospital)

Data availability The experiment data is available upon request.

References

1. Lexau SJ, Breivik M, Lekkas AM (2023) Automated docking for marine surface vessels—a survey. IEEE Access 11:132324–132367
2. Eliopoulou E, Papanikolaou A, Voulgarellis M (2016) Statistical analysis of ship accidents and review of safety level. Saf Sci 85:282–292
3. Weng J, Yang D, Qian T, Huang Z (2018) Combining zero-inflated negative binomial regression with mlrt techniques: an approach to evaluating shipping accident casualties. Ocean Eng 166:135–144
4. Wang H, Li X, Chen L, Sun X (2016) Numerical study on the hydrodynamic forces on a ship berthing to quay by taking free-surface effect into account. J Mar Sci Technol 21:601–610
5. Bitar G, Martinsen AB, Lekkas AM, Breivik M (2020) Trajectory planning and control for automatic docking of ASVs with full-scale experiments. IFAC-PapersOnLine 53:14488–14494
6. Rachman DM, Maki A, Miyauchi Y, Umeda N (2022) Warm-started semionline trajectory planner for ship's automatic docking (berthing). Ocean Eng 252:111127
7. Xia Z, Guo Z, Wang W, Jiang Y (2021) Joint optimization of ship scheduling and speed reduction: A new strategy considering high transport efficiency and low carbon of ships in port. Ocean Eng 233:109224
8. Cho Y, Han J, Kim J (2020) Efficient colreg-compliant collision avoidance in multi-ship encounter situations. IEEE Trans Intell Transp Syst 23:1899–1911
9. Fossen T (2021) Handbook of marine craft hydrodynamics and motion control, 2nd edn. Wiley
10. Sørensen AJ (2011) A survey of dynamic positioning control systems. Annu Rev Control 35:123–136
11. Guo S, Zhang X, Zheng Y, Du Y (2020) An autonomous path planning model for unmanned ships based on deep reinforcement learning. Sensors 20:426
12. Zhao Y et al (2020) Path following optimization for an under-actuated usv using smoothly-convergent deep reinforcement learning. IEEE Trans Intell Transp Syst 22:6208–6220
13. Shimizu S et al (2022) Automatic berthing using supervised learning and reinforcement learning. Ocean Eng 265:112553
14. Ahmed YA, Hasegawa K (2013) Automatic ship berthing using artificial neural network trained by consistent teaching data using nonlinear programming method. Eng Appl Artif Intell 26:2287–2304
15. Im N-K, Nguyen V-S (2018) Artificial neural network controller for automatic ship berthing using head-up coordinate system. Int J Naval Arch Ocean Eng 10:235–249
16. Haseltalab A, Negenborn RR (2019) Adaptive control for autonomous ships with uncertain model and unknown propeller dynamics. Control Eng Pract 91:104116
17. Skulstad R, Li G, Fossen TI, Vik B, Zhang H (2020) A hybrid approach to motion prediction for ship docking-integration of a neural network model into the ship dynamic model. IEEE Trans Instrum Meas 70:1–11

18. Martinsen AB, Lekkas AM, Gros S (2019) Autonomous docking using direct optimal control. IFAC-PapersOnLine 52:97–102
19. Li D-J, Chen Y-H, Shi J-G, Yang C-J (2015) Autonomous underwater vehicle docking system for cabled ocean observatory network. Ocean Eng 109:127–134
20. Teo K, An E, Beaujean P-PJ (2012) A robust fuzzy autonomous underwater vehicle (AUV) docking approach for unknown current disturbances. IEEE J Oceanic Eng 37:143–155
21. Teo K, Goh B, Chai OK (2014) Fuzzy docking guidance using augmented navigation system on an AUV. IEEE J Oceanic Eng 40:349–361
22. Fan S, Liu C, Li B, Xu Y, Xu W (2019) AUV docking based on USBL navigation and vision guidance. J Mar Sci Technol 24:673–685
23. Smogeli O, Trong N, Borhaug B, Pivano L (2013) The next level DP capability analysis. In: Dynamic Positioning Conference, pp 15–16
24. Sawada R et al (2021) Path following algorithm application to automatic berthing control. J Mar Sci Technol 26:541–554
25. SNAME (1950) Nomenclature for treating the motion of a submerged body through a fluid: report of the American towing tank conference. In: The Society of Naval Architects and Marine Engineers, Technical and Research Bulletin
26. Walmsness JE, Helgesen HH, Larsen S, Kufoalor GKM, Johansen TA (2023) Automatic dock-to-dock control system for surface vessels using bumpless transfer. Ocean Eng 268:113425
27. Pedersen AA (2019) Optimization based system identification for the milliAmpere ferry. Master's thesis, NTNU
28. Torben TR, Brodtkorb AH, Sørensen AJ (2020) Control allocation for double-ended ferries with full-scale experimental results. Int J Control Autom Syst 18:556–563
29. Zaccarian L, Teel AR (2002) A common framework for anti-windup, bumpless transfer and reliable designs. Automatica 38:1735–1744
30. Teel AR, Kapoor N (1997) The L2 anti-winup problem: Its definition and solution. In: 1997 European Control Conference (ECC), pp 1897–1902
31. Fossen TI, Perez T (2009) Kalman filtering for positioning and heading control of ships and offshore rigs. IEEE Control Syst Mag 29:32–46
32. Stephens R (2011) Wind feedforward: blowing away the myths. In: *Marine Technology Society Dynamic Positioning Conference*
33. Chen Z, Yu J, Zhao Z, Wang X, Chen Y (2023) A path-planning method considering environmental disturbance based on VPF-RRT. Drones 7:145
34. Wang N, Zhang Y, Ahn CK, Xu Q (2021) Autonomous pilot of unmanned surface vehicles: Bridging path planning and tracking. IEEE Trans Veh Technol 71:2358–2374